Design of an Intake and a Thruster for an Atmosphere-Breathing Electric Propulsion System

F. Romano[a,b,1], G. Herdrich[b], Y.-A. Chan[b], N.H. Crisp[c], P.C.E. Roberts[c],
B. E.A. Holmes[c], S. Edmondson[c], S. Haigh[c], A. Macario-Rojas[c],
V.T. A. Oiko[c], L.A. Sinpetru[c], K. Smith[c], J. Becedas[d], V. Sulliotti-Linner[d],
M. Bisgaard[e], S. Christensen[e], V. Hanessian[e], T. Kauffman Jensen[e],
J. Nielsen[e], S. Fasoulas[b], C. Traub[b], D. García-Almiñana[f],
S. Rodríguez-Donaire[f], M. Sureda[f], D. Kataria[g], B. Belkouchi[h], A. Conte[h],
S. Seminari[h], R. Villain[h]

[a]*Ecole Polytechnique Fédérale de Lausanne (EPFL), Swiss Plasma Center (SPC), CH-1015 Lausanne, Switzerland*
[b]*Institute of Space Systems (IRS), University of Stuttgart, 70569, Germany*
[c]*The University of Manchester, Oxford Road, Manchester, M13 9PL, UK*
[d]*Elecnor Deimos Satellite Systems, C/ Francia 9, 13500, Puertollano, Spain*
[e]*GomSpace AS, Langagervej 6, Aalborg East 9220, Denmark*
[f]*UPC-BarcelonaTECH, Colom 11, TR5 - 08222 Terrassa, Spain*
[g]*Mullard Space Science Laboratory, University College London, Holmbury St. Mary, Dorking, Surrey, RH5 6NT, UK*
[h]*Euroconsult, 86 Boulevard de Sébastopol, 75003 Paris, France*

Abstract

Challenging space missions include those at very low altitudes, where the atmosphere is the source of aerodynamic drag on the spacecraft, that finally defines the mission's lifetime, unless a way to compensate for it is provided. This environment is named Very Low Earth Orbit (VLEO) and it is defined for $h < 450\,\text{km}$. In addition to the spacecraft's aerodynamic design, to extend the lifetime of such missions, an efficient propulsion system is required.

One solution is Atmosphere-Breathing Electric Propulsion (ABEP), in which the propulsion system collects the atmospheric particles to be used as propellant for an electric thruster. The system could remove the requirement of carrying propellant on-board, and could also be applied to any planetary body with atmosphere, enabling new missions at low altitude ranges for longer missions' duration. One of the objectives of the H2020 DISCOVERER project, is the development of an intake and an electrode-less plasma thruster for an ABEP system.

This article describes the characteristics of intake design and the respective final designs based on simulations, providing collection efficiencies up to 94%. Furthermore, the radio frequency (RF) Helicon-based plasma thruster (IPT) is hereby presented as well, while its performances are being evaluated, the

---

[1]Postdoctoral Researcher, francesco.romano@epfl.ch

IPT has been operated with single atmospheric species as propellant, and has highlighted very low input power requirement for operation at comparable mass flow rates $P \sim 60\,\mathrm{W}$.

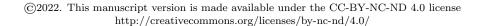**Keywords:** ABEP - Intake - VLEO - Birdcage - Helicon

Nomenclature

ABEP: Atmosphere-Breathing Electric Propulsion
DSMC: Direct Simulation Monte Carlo
FMF: Free Molecular Flow
GSI: Gas-Surface Interaction
IPT: RF Helicon-based Plasma Thruster
VLEO: Very Low Earth Orbit
SC: Spacecraft

1. Introduction

1.1. ABEP Concept

An atmosphere-breathing electric propulsion system (ABEP), see Fig. 1, is mainly made of two components: the intake and the electric thruster. The system is designed for spacecrafts (SCs) orbiting at very low altitude orbits, for example in very low Earth orbit (VLEO), defined for altitudes $h < 450\,\mathrm{km}$ [1]. The ABEP system collects the residual atmospheric particles encountered by the SC through the intake and uses them as propellant for the electric thruster. The system is theoretically applicable to any planetary body with an atmosphere, and can drastically reduce the on-board propellant storage requirement, while extending the mission's lifetime [2]. Many ABEP concepts have been investigated in the past based on radio frequency ion thrusters (RIT) [3–12], ECR-based thruster [13–17], Hall-effect thrusters (HET) [18–25], and plasma thrusters [26]. The only laboratory tested ABEP systems to date are the ABIE developed in Japan, composed of an annular intake and an ECR-based thruster into one device [13–16], and the RAM-HET system developed in Europe, comprised of the intake and a HET assembled into one device [20–24]. Current research in Europe is developed within the H2020 DISCOVERER and AETHER projects.
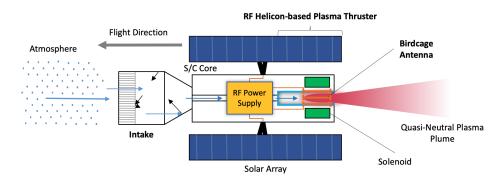
2

Figure 1: Atmosphere-Breathing Electric Propulsion Concept using the RF Helicon-based Plasma Thruster (IPT) [27].

1.2. Very Low Earth Orbit

The ABEP operational environment is the VLEO altitude range, that can be described by mainly density and composition over altitude and location based on atmospheric models. Among the several available, the NRLMSISE-00 is used as it accurately accounts for the lower thermosphere atmospheric conditions, as well as for being used for previous work on ABEP systems [2, 28, 29]. In Fig. 2, the averaged particle number densities are plotted in VLEO for an equatorial orbit - an aspect that fosters relevant verifications on level of the comparison between different studies.
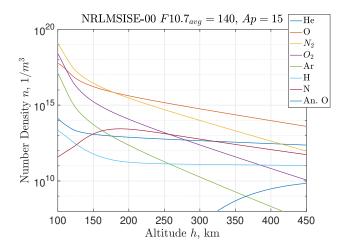

Figure 2: Atmospheric Composition in VLEO, NRLMSISE-00 Atmospheric Model: $F10.7 = 140$, $Ap = 15$, Moderate Solar Activity.

The solar activity is set as moderate with a respective $F10.7 = 140$, the solar radio flux at a wavelength of $\lambda = 10.7\,\mathrm{cm}$, and the geomagnetic index $Ap = 15$. The ABEP altitudes range is set to $h = 150 - 250\,\mathrm{km}$. The lower limit is due to aerodynamic drag, as it increases exponentially leading to large

power requirements [29] and also heating of the SC [2]. The upper limit is set by the limited propellant collection, that can become lower than conventional thruster requirements by a typical sized SC, and is where a conventional electric propulsion system becomes preferable against an ABEP system [3]. The dominant gas species in the selected altitude range are N_2 and atomic oxygen (AO).

It is very important to mention, that an ABEP system must be able to perform in a wide operational envelope of parameters. Indeed, a variable incoming propellant composition and flow is expected, that also translates in larger or lower values of aerodynamic drag. This is in particular due to the non-uniformity of VLEO environment because of temporal (time), seasonal (solar activity), and geographical (latitude and longitude) variations. Also, one must take into account for more expectional space weather events, such high energetic particle fluxes coming from the Sun due to, for example, UV or X-ray flares. Such effects would change the drag, therefore the thrust requirements, as well as the propellant composition and, therefore, the power requirements, and need to be taken into account for the system's design. A more detailed analysis can be found in [30, 31].

2. ABEP Intake

2.1. Intake Working Principle

The intake is the device of an ABEP system that collects and drives the atmospheric particles to the thruster. The general schematics is shown in Fig. 3. The intake shall ensure the efficient collection of atmospheric particles and provide the required conditions of density, pressure, and mass flow for thruster's operation while, at the same time, minimizing the required frontal area and, therefore, the resulting drag.
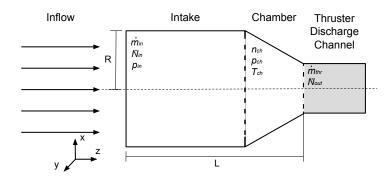

Figure 3: Intake General Design including the Thruster's Discharge Channel [32].

The number density is n and $\dot{N}$ is the particle flux. The collection efficiency $\eta_c(h)$ is defined in Eq. 1, where $\dot{N}_{out}$ is the collected particle flux, and $\dot{N}_{in}$ is the

incoming one. The subscript i refers to each different particle species $i = [1, N_s]$, where N_s is the total number of species.

$$\eta_c(h) = \frac{\sum_{i=1}^{N_s} \dot{N}_{out_i}}{\sum_{i=1}^{N_s} \dot{N}_{in_i}} \tag{1}$$

The resulting mass flow to the thruster $\dot{m}_{thr}$ is obtained as shown in Eq. 2, where m_p is the particle mass.

$$\dot{m}_{thr}(h) = \sum_{i=1}^{N_s} m_{p_i} \, \dot{N}_{out_i}(h) \tag{2}$$

It shall be noted that each intake design needs to be tailored to the thruster applied, its requirements, and the mission profile. The latter, in terms of orbit (altitude and inclination), and total mission duration to account for solar activity variations.

Intake design, due to the free molecular flow condition in VLEO, is mostly driven by gas-surface interaction (GSI) properties of the materials [33]. Based on the Maxwell's model, upon particle impact with a surface, an exchange of momentum and energy takes place. In this model, two types of surface-particle interactions are modelled: specular and diffuse reflections. In specular reflections, particles are reflected without energy exchange, the angle of reflection equals the incident angle, and the velocity vector undergoes a complete inversion. In diffuse reflection, instead, particles reach thermal equilibrium with the surface and are reflected according to a Rayleigh distribution corresponding to the wall temperature T_{wall} with only thermal velocity.

The accommodation coefficient α is defined in Eq. 3, where the energy of the incident particle is E, and E' the energy of the reflected particle, while E_W is the energy which a particle would have after full accommodation to T_{wall}. For specular reflections, $\alpha = 1$, while for diffuse ones is $\alpha = 0$.

$$\alpha = \frac{E - E'}{E - E_W} \tag{3}$$

The intakes hereby presented have been designed using the PICLas tool, which is a three-dimensional numerical tool for simulating non-equilibrium gas and plasma flows [34, 35]. For the intake design, the DSMC module with the Maxwell model for surface interactions is used [32]. Details on the inflow parameters, that are based on NRLMSISE-00 model at moderate solar activity, can be found in [30, 32].

2.2. Diffuse Intake

Based on the analysis of the intake concepts using diffuse scattering $\alpha = 0$, this design provides a homogenous pressure distribution in front of the thruster's discharge channel as shown in Fig. 4. The intake has an hexagonal shape and it features a front section of hexagonal ducts with different area ratio AR: larger ducts in front of the thruster's discharge channel to increase A_{in}, and narrower

ones in the outer intake region to reduce the backflow. At the rear there is a conical section with a chamber angle of 45° terminating on the thruster's discharge channel diameter. In Fig. 5 the isometric render view of the diffuse intake is shown. This design provides a theoretical maximum of $\eta_c = 0.458$ [32].
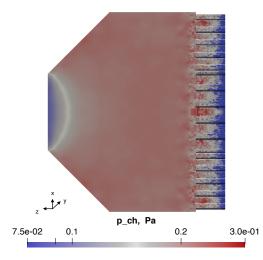

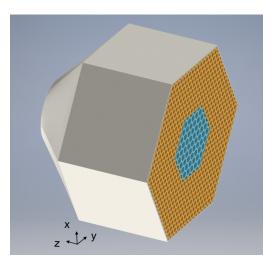Figure 4: Diffuse Intake Pressure Distribution [32].

Figure 5: Diffuse Intake Render [32].

2.3. Specular Intake

Based on specular scattering properties $\alpha = 1$, a parabolic scoop with its focus inside the thruster discharge channel provides a theoretical $\eta_c = 0.94$ [32]. This design also outperforms the diffuse intake in terms of sensitivity to flow

misalignment leading to a limit of $\alpha = 15°$ resulting in $\eta_c < 0.6$. The isometric render view of the specular intake is shown in Fig. 7 [32].
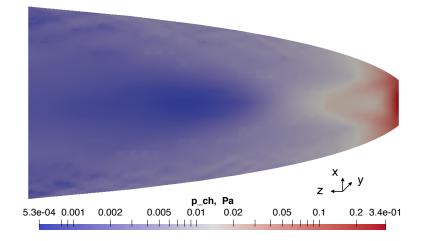

Figure 6: Specular Intake Pressure Distribution [32].
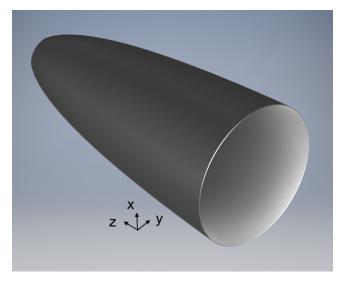

Figure 7: Specular Intake Render [32].

3. ABEP Thruster

3.1. Thruster Working Principle

The thruster concept is based on an antenna fed by a RF power which ionizes and accelerates the propellant. In particular, the antenna surrounds a

dielectric discharge channel, in which the propellant is injected. The RF-fed antenna launches electromagnetic waves within the discharge channel exciting the propellant particles: it ionizes them and, in combination with an externally applied magnetic field, that is provided by either a solenoid or a system of permanent magnets, accelerates them through the exhaust producing thrust, see Fig. 8.
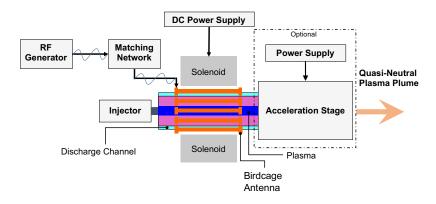

Figure 8: RF Helicon-based Plasma Thruster (IPT) Concept [27].

Furthermore, the applied magnetic field also provides one of the required boundary conditions for helicon waves to develop in the plasma, therefore improving the discharge efficiency [36].

3.2. RF Helicon-based Plasma Thruster (IPT)

The RF Helicon-based plasma thruster (IPT) is a contact-less device based on a novel antenna type, the birdcage antenna. Such an antenna has the advantage of operating at a specific resonance mode that provides not only an already matched load to the RF circuit, but also a linearly polarized magnetic (and electric) field within the IPT's discharge channel. The first property leads to an optimum electrical performance by maximizing the power transfer efficiency, therefore, minimizing losses and heating. The second, the linearly polarized electric and magnetic field, theoretically provides a drift velocity to both ions and electrons along the axial direction due to the $\vec{E} \times \vec{B}$ product that is independent of the particle charge [27, 30]. The IPT is protected/and protects the outer environment from RF waves by means of a Faraday cage made by of brass placed around the birdcage antenna itself. Around the IPT, in the antenna region, a solenoid provides up to $B < 70\,\mathrm{mT}$ of static magnetic field at the axis, that enhances the plasma discharge by providing one of the boundary conditions for the formation of helicon waves within the plasma itself [30, 36]. Furthermore, the magnetic field divergence at the exhaust of the IPT provides a magnetic nozzle effect for thrust production, along with the drift velocity given by the birdcage antenna. The RF Helicon-based plasma thruster (IPT) has been simulated, designed, and built for an operational frequency of

8

$f = 40.68\,\mathrm{MHz}$. The experimental set-up is composed by an Advanced Energy CESAR 4040 $f = 40.68\,\mathrm{MHz}$ RF generator, an Advanced Energy Navigator 4040-L70 automatic matching network, the electromagnet is fed by a GENSYS 750 W DC power supply, and the IPT itself is flanged to the vacuum chamber. The vacuum chamber has a diameter of $D = 1\,\mathrm{m}$ and a length of $L = 2.75\,\mathrm{m}$. The vacuum pumping system provides a final base pressure of $p < 0.01\,\mathrm{Pa}$.

The electrical performances have been verified experimentally against simulations in terms of impedance and resonance frequency [27, 30], and the IPT was successfully demonstrated to operate on Ar as well as atmospheric gases such as N_2 and O_2, in particular ignition, operation at minimum reflected power, and formation of a visible collimated plasma plume in the vacuum chamber after applying the external magnetic field [30]. The assembled IPT is shown in Fig. 9, and its operation on Ar, N_2, and O_2 is shown in Fig. 10, where the particle flux, power input, and applied magnetic field are equal for the three cases. The three pictures are taken through an optical window with identical camera settings.
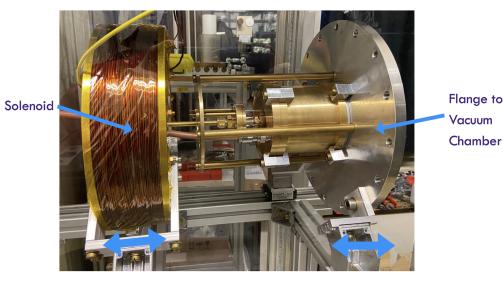

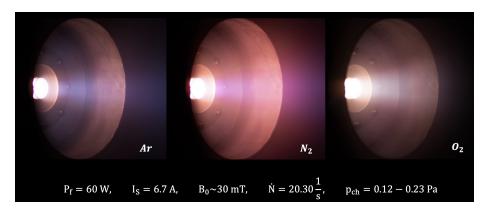Figure 9: RF Helicon-based Plasma Thruster (IPT) Prototype.

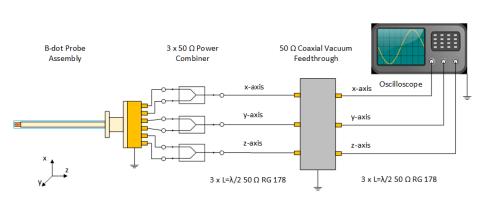Figure 10: RF Helicon-based Plasma (IPT) in Operation.

4. Diagnostic for Thruster Development

To further develop the IPT, specific diagnostics are required to evaluate the discharge behaviour as well as to determine the thrust produced. First, a scientific evidence of formation of helicon waves is of high interest to highlight the effective operation of the IPT in the helicon regime [37, 38]. This can be achieved by employing a 3-axis magnetic-inductive B-dot probe that is currently undergoing calibration at IRS. Such probe allows the measurement of the rotating magnetic field that is typical of helicon waves in the plasma plume [30, 39].

The probe shown in Fig. 11, is made of three small $N = 5$ turns coils with $\phi = 0.2\,\text{mm}$ wire, and a coil area respectively of $A_x = 16\,\text{mm}^2$, $A_y = 25\,\text{mm}^2$, and $A_z = 36\,\text{mm}^2$, that can detect the time-varying magnetic fields as they induce a voltage V at an angular frequency $\omega = 2\pi f$, see Eq. 4.

$$V = -NA\left|\frac{dB_{tot}}{dt}\right| = -NA\omega|B| \tag{4}$$

The probe material is mainly PEEK due to mechanical strength and relatively high melting temperature. An additional quartz cover is added to shield the probe from the direct plasma bombardment. The signal measured by each coil is sent to RF power combiners (one per axis) to remove capacitive pick-up that arises between plasma and coils, see Fig. 11.

Figure 11: Magnetic Inductive B-dot Probe.

To directly measure the produced thrust, isntead, a thrust/force balance is required.

Such device is a mechanical structure that is capable to isolate the thrust force from the external forces, and to translate it into a displacement that can be measured. A schematics of a typical pendulum-type thrust balance set-up is shown within Fig. 12. The pendulum-type is made by the thruster (e) mounted at the bottom of an arm (d) that can oscillate around its center thanks to a bearing (b). On the other side of the arm there is a damper (a), whereas a translation sensor (c) is mounted close to the center of the arm to measure the movement due to the thruster operation.

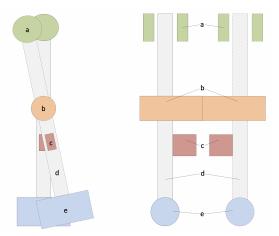

Figure 12: Example of a Pendulum-Type Thrust Balance: a) damper, b) bearing, c) translation sensor, d) pendulum arm structure, e) thruster [40].

To perform such measurement, the current version of the IPT needs to be upgraded and optimized to allow vacuum operation and mounting on the thrust balance, therefore reducing the weight, in particular of the solenoid for the applied magnetic field.

5. Conclusion

This article provides the design of the intake and the thruster for an ABEP system. The working principle ABEP intakes based on diffuse and specular-based GSI properties is presented, and highlights the advantages of the specular intake in terms of both intake efficiency, $\eta_c = 0.94$, and robustness of its performance to misalignment with the free stream [32]. However, the diffuse intake design providing $\eta_c = 0.458$, is still applicable due also to its larger higher-pressure region provided. Finally, the selection always depends on the mission requirements [32].

The RF Helicon-based plasma thruster (IPT) is based on RF contact-less technology using an innovative birdcage antenna that allows to minimize power requirement while enhancing thruster operation. The IPT does not have any component in direct contact with the plasma that could erode, critical for ABEP application due to the presence of atomic oxygen (AO), and it does not require a neutralizer as the plasma plume ejected is quasi-neutral. The IPT electrical properties have been experimentally verified [27, 30], and its proof of concept achieved by operating it on Ar as well as on N_2 and O_2 [30, 39, 41].

Currently, a set of sub-scale intake prototypes are being prepared to test in the Rarefied Orbital Aerodynamics Research facility (ROAR) at The University of Manchester [42] developed within the H2020 DISCOVERER project, creating relevant VLEO AO flow conditions. Also, the future incoming results on the measurements of aerodynamic coefficients from the Satellite for Orbital Aerodynamics Research (SOAR) [43] will be used as well. The application of real material GSI properties to the simulations is necessary to reach the first full intake prototypes.

The IPT will undergo a first set of diagnostics to provide a first thrust measurement by a momentum flux probe that is in the development phase. In parallel the detection of helicon waves within the plasma plume is to be performed by applying a magnetic inductive 3-axes B-dot probe that is currently undergoing calibrations [30, 39, 41]. A full RF-compensated plasma diagnostic measurement is to be performed for fully characterise the IPT. In the near future, a vacuum-capable IPT version is to be developed for later performing direct thrust measurement by means of a thrust pendulum.

Finally, the intake design work is strongly linked (and iterated) with the thruster design work, to ensure their operation in a common range of pressures, mass flows, and efficiencies. Therefore, both intake and thruster development will mutually feed into each other for the final ABEP complete system design that, once again, is strongly linked to the detailed mission profile as well, but must always allow the operation in a variable environment.

Acknowledgements

flects only the author's view and the European Commission is not responsible for any use that may be made of the information it contains.

References

[1] P. Roberts, N. Crisp, V. Abrao Oiko, S. Edmondson, S. Haigh, C. Huyton, S. Livadiotti, R. Lyons, K. Smith, L. Sinpetru, A. Straker, S. Worrall, F. Romano, G. Herdrich, A. Boxberger, Y.-A. Chan, C. Traub, S. Fasoulas, K. Smith, R. Outlaw, J. Becedas, R. Domínguez, D. González, V. Hanessian, A. Mølgaard, J. Nielsen, M. Bisgaard, D. Garcia-Almiñana, S. Rodriguez-Donaire, M. Sureda, D. Kataria, R. Villain, J. S. Perez, A. Conte, B. Belkouchi, A. Schwalber, B. Heißerer, DISCOVERER – making commercial satellite operations in very low Earth orbit a reality, 70th International Astronautical Congress, Washington D.C., USA (IAC-19.C2.6.1x50774) (October 2019).

[2] F. Romano, B. Massuti-Ballester, T. Binder, G. Herdrich, S. Fasoulas, T. Schönherr, System analysis and test-bed for an atmosphere-breathing electric propulsion system using an inductive plasma thruster, Acta Astronautica 147 (2018) 114 – 126. doi:https://doi.org/10.1016/j.actaastro.2018.03.031.

[3] D. Di Cara, J. Gonzalez del Amo, A. Santovincenzo, B. C. Domínguez, M. Arcioni, A. Caldwell, I. Roma, RAM electric propulsion for low Earth orbit operation: an ESA study, 30th International Electric Propulsion Conference 2007, Florence, Italy (IEPC 2007 162) (September 2007).

[4] G. Cifali, T. Misuri, P. Rossetti, M. Andrenucci, D. Valentian, D. Feili, B. Lotz, Experimental characterization of HET and RIT with atmospheric propellants, 32nd International Electric Propulsion Conference, Wiesbaden, Germany (IEPC 2011 224) (September 2011).

[5] G. Cifali, D. Dignani, T. Misuri, P. Rossetti, M. Andrenucci, D. Valentian, F. Marchandise, D. Feili, B. Lotz, Completion of HET and RIT characterization with atmospheric propellants, Space Propulsion 2012, Bordeaux, France (SP2012 2355386) (May 2012).

[6] A. Fitatyev, A. Golikov, L. Nosachev, V. Skvortsov, D. Padalitsa, Spacecraft with air-breathing electric propulsion as the future ultra-speed aircraft, 71st International Astronautical Congress, Online, The CyberSpace Edition (IAC-20,C4,6,8,x59643) (October 2020).

[7] A. Erofeev, A. Nikiforov, G. Popov, M. Suvorov, S. Syrin, S. Khartov, Air-breathing ramjet electric propulsion for controlling low-orbit spacecraft motion to compensate for aerodynamic drag, Solar System Research 51 (7) (2017) 639–645.

[8] A. S. Filatyev, O. V. Yanova, The control optimization of low-orbit spacecraft with electric ramjet, Acta Astronautica 158 (2019) 23–31.

13

[9] M. Y. Marov, A. S. Filatyev, Integrated studies of electric propulsion engines during flights in the earth's ionosphere, Cosmic Research 56 (2) (2018) 123–129. doi:10.1134/S0010952518020041.

[10] A. I. Erofeev, Air intake in the transient regime of rarefied gas flow, TsAGI Science Journal 49 (2) (2018).

[11] A. Erofeev, A. Nikiforov, G. Popov, M. Suvorov, S. Syrin, S. Khartov, Air-breathing ramjet electric propulsion for controlling low-orbit spacecraft motion to compensate for aerodynamic drag, Solar System Research 51 (7) (2017) 639–645.

[12] S. Kanev, V. Petukhov, G. Popov, S. Khartov, Electro-rocket ramjet thruster for compensating the aerodynamic drag of a low-orbit spacecraft, Russian Aeronautics (Iz VUZ) 58 (3) (2015) 286–291.

[13] K. Fujita, Air intake performance of air breathing ion engines, Journal of the Japan Society for Aeronautical and Space Sciences 52 (610) (2004) 514–521. doi:10.2322/jjsass.52.514.

[14] K. Fujita, Air-intake performance estimation of air-breathing ion engines, Transactions of the Japan Society of Mechanical Engineers. B 70 (700) (2004) 3038–3044.

[15] Y. Hisamoto, K. Nishiyama, H. Kuninaka, Development statue of atomic oxygen simulator for air breathing ion engine, in: 32nd Intern. Electric Propulsion Conference. IEPC 2011 (Wiesbaden, Germany, Sept. 11-15 2011): Proc, 2011.

[16] Y. Hisamoto, K. Nishiyama, H. Kuninaka, Design of air intake for air breathing ion engine, in: 63rd International Astronautical Congress, no. IAC-12,C4,4,10,x14578, 2012.

[17] M. Tagawa, K. Yokota, K. Nishiyama, H. Kuninaka, Y. Yoshizawa, D. Yamamoto, T. Tsuboi, Experimental study of air breathing ion engine using laser detonation beam source, Journal of Propulsion and Power 29 (3) (2013) 501–506. doi:10.2514/1.B34530.

[18] K. Hohman, Atmospheric breathing electric thruster for planetary exploration, Busek Co. Inc. 11 (2012) 01760–1023.

[19] K. Hohman, Atmospheric breathing electric thruster for planetary exploration, Presented as the NIAC Spring Symposium, Presentation, 2012.

[20] S. Barral, G. Cifali, R. Albertoni, M. Andrenucci, L. Walpot, Conceptual design of an air-breathing electric propulsion system, in: Joint Conf. of 30th Int. Symp. on Space Technology and Science, 34th Int. Electric Propulsion Conf. and 6th Nano-Satellite Symp, 2015.

[21] G. Cifali, T. Andrenussi, V. Giannetti, A. Leoprini, A. Rossodivita, M. Andrenucci, S. Barral, J. Longo, L. Walpot, Experimental validation of a RAM-EP concept based on Hall-effect thruster, Space Propulsion 2016, Rome, Italy (SP2016 3125202) (May 2016).

[22] T. Andreussi, G. Cifali, V. Giannetti, A. Piragino, E. Ferrato, A. Rossodivita, M. Andrenucci, J. Longo, L. Walpot, Development and experimental validation of a Hall-effect thruster RAM-EP concept, 35th International Electric Propulsion Conference, Atlanta, USA (IEPC 2017 377) (October 2017).

[23] T. Andreussi, E. Ferrato, V. Giannetti, A. Piragino, C. A. Paissoni, G. Cifali, M. Andrenucci, Development status and way forward of SITAEL's air-breathing electric propulsion engine, in: AIAA Propulsion and Energy 2019 Forum, 3996, 2019.

[24] E. Ferrato, V. Giannetti, A. Piragino, M. Andrenucci, T. Andreussi, C. A. Paissoni, Development roadmap of SITAEL's RAM-EP system, 36th International Electric Propulsion Conference, Vienna, Austria (IEPC 2019 886) (September 2019).

[25] D. V. Dukhopelnikov, V. A. Riazanov, S. O. Shilov, D. S. Manegin, R. A. Sokolov, Investigation of the laboratory model of a thruster with anode layer operating with air and nitrogen-oxygen mixture, AIP Conference Proceedings 2318 (1) (2021) 040006. doi:10.1063/5.0036251.

[26] A. Shabshelowitz, Study of RF plasma technology applied to air-breathing electric propulsion, Ph.D. thesis, University of Michigan (2013).

[27] F. Romano, Y.-A. Chan, G. Herdrich, C. Traub, S. Fasoulas, P. Roberts, K. Smith, S. Edmondson, S. Haigh, N. Crisp, V. Oiko, S. Worrall, S. Livadiotti, C. Huyton, L. Sinpetru, A. Straker, J. Becedas, R. Domínguez, D. González, V. Cañas, V. Sulliotti-Linner, V. Hanessian, A. Mølgaard, J. Nielsen, M. Bisgaard, D. Garcia-Almiñana, S. Rodriguez-Donaire, M. Sureda, D. Kataria, R. Outlaw, R. Villain, J. Perez, A. Conte, B. Belkouchi, A. Schwalber, B. Heißerer, RF Helicon-based Inductive Plasma Thruster (IPT) Design for an Atmosphere-Breathing Electric Propulsion system (ABEP), Acta Astronautica 176 (2020) 476 – 483. doi:https://doi.org/10.1016/j.actaastro.2020.07.008.

[28] M. Leomanni, A. Garulli, A. Giannitrapani, F. Scortecci, Propulsion options for very low earth orbit microsatellites, Acta Astronautica 133 (2017) 444–454. doi:https://doi.org/10.1016/j.actaastro.2016.11.001.

[29] T. Schönherr, K. Komurasaki, F. Romano, B. Massuti-Ballester, G. Herdrich, Analysis of atmosphere-breathing electric propulsion, Plasma Science, IEEE Transactions on 43 (1) (2015) 287–294. doi:10.1109/TPS.2014.2364053.

[30] F. Romano, RF Helicon Plasma Thruster for an Atmosphere-Breathing Electric Propulsion System (ABEP), Verlag Dr. Hut, 2022.

[31] S. Vaidya, C. Traub, F. Romano, G. Herdrich, Y.-A. Chan, S. Fasoulas, P. Roberts, N. Crisp, S. Edmondson, S. Haigh, et al., Development and analysis of novel mission scenarios based on atmosphere-breathing electric propulsion (ABEP), CEAS Space Journal (2022) 1–18doi:10.1007/s12567-022-00436-1.

[32] F. Romano, J. Espinosa-Orozco, M. Pfeiffer, G. Herdrich, N. Crisp, P. Roberts, B. Holmes, S. Edmondson, S. Haigh, S. Livadiotti, A. Macario-Rojas, V. Oiko, L. Sinpetru, K. Smith, J. Becedas, V. Sulliotti-Linner, M. Bisgaard, S. Christensen, V. Hanessian, T. K. Jensen, J. Nielsen, Y.-A. Chan, S. Fasoulas, C. Traub, D. García-Almiñana, S. Rodríguez-Donaire, M. Sureda, D. Kataria, B. Belkouchi, A. Conte, S. Seminari, R. Villain, Intake design for an Atmosphere-Breathing Electric Propulsion system (ABEP), Acta Astronautica 187 (2021) 225–235. doi:10.1016/j.actaastro.2021.06.033.

[33] S. Livadiotti, N. H. Crisp, P. C. Roberts, S. D. Worrall, V. T. Oiko, S. Edmondson, S. J. Haigh, C. Huyton, K. L. Smith, L. A. Sinpetru, B. E. Holmes, J. Becedas, R. M. Domínguez, V. Cañas, S. Christensen, A. Mølgaard, J. Nielsen, M. Bisgaard, Y.-A. Chan, G. H. Herdrich, F. Romano, S. Fasoulas, C. Traub, D. Garcia-Almiñana, S. Rodriguez-Donaire, M. Sureda, D. Kataria, B. Belkouchi, A. Conte, J. S. Perez, R. Villain, R. Outlaw, A review of gas-surface interaction models for orbital aerodynamics applications, Progress in Aerospace Sciences 119 (2020) 100675. doi:10.1016/j.paerosci.2020.100675.

[34] C.-D. Munz, M. Auweter-Kurtz, S. Fasoulas, A. Mirza, P. Ortwein, M. Pfeiffer, T. Stindl, Coupled particle-in-cell and direct simulation monte carlo method for simulating reactive plasma flows, Comptes Rendus Mécanique 342 (10–11) (2014) 662 – 670, theoretical and numerical approaches for Vlasov-maxwell equations. doi:http://dx.doi.org/10.1016/j.crme.2014.07.005.

[35] S. Fasoulas, C.-D. Munz, M. Pfeiffer, J. Beyer, T. Binder, S. Copplestone, A. Mirza, P. Nizenkov, P. Ortwein, W. Reschke, Combining particle-in-cell and direct simulation monte carlo for the simulation of reactive plasma flows, Physics of Fluids 31 (7) (2019) 072006. doi:10.1063/1.5097638.

[36] F. F. Chen, Helicon discharges and sources: a review, Plasma Sources Science and Technology 24 (1) (2015) 014001. doi:10.1088/0963-0252/24/1/014001.

[37] R. Jacquier, R. Agnello, B. P. Duteil, P. Guittienne, A. Howling, G. Plyushchev, C. Marini, A. Simonin, I. Morgal, S. Bechu, et al., First B-dot measurements in the RAID device, an alternative negative ion

source for demo neutral beams, Fusion Engineering and Design (2019). doi:https://doi.org/10.1016/j.fusengdes.2019.02.025.

[38] P. Guittienne, R. Jacquier, B. P. Duteil, A. A. Howling, R. Agnello, I. Furno, Helicon wave plasma generated by a resonant birdcage antenna: magnetic field measurements and analysis in the RAID linear device, Plasma Sources Science and Technology 30 (7) (2021) 075023. doi:10.1088/1361-6595/ac0da3.

[39] F. Romano, Y.-A. Chan, G. Herdrich, C. Traub, S. Fasoulas, P. Roberts, N. Crisp, B. Holmes, S. Edmonson, S. Haigh, S. Livadiotti, A. Macario-Rojes, V. Oiko, L. Sinpetru, K. Smith, J. Becedas, V. Sulliotti-Linner, M. Bisgaard, S. Christensen, V. Hanessian, T. K. Jensen, J. Nielsen, D. Garcia-Almiñana, M. G.-B. S. Rodrigue-Donaire, M. Sureda, D. Kataria, B. Belkouchi, A. Conte, S. Seminari., Design, set-up, and first ignition of the RF Helicon-based Plasma Thruster, Space Propulsion 2021, Online (SP2021 00247) (March 2021).

[40] F. G. Hey, A. Keller, C. Braxmaier, M. Tajmar, U. Johann, D. Weise, Development of a highly precise micronewton thrust balance, IEEE Transactions on Plasma Science 43 (1) (2014) 234–239.

[41] F. Romano, G. Herdrich, , Y.-A. Chan, P. C. Roberts, N. H. Crisp, A. Macario Rojas, S. Edmondson, S. Haigh, B. Holmes, S. Livadiotti, V. A. Oiko, K. Smith, L. Sinpetru, J. Becedas, R. Domínguez, V. Sulliotti-Linne, S. Christensen, T. Kauffman Jensen, J. Nielsen, M. Bisgaard, S. Fasoulas, C. Traub, D. Garcia-Almiñana, M. Garcia-Berenguer, S. Rodriguez-Donaire, M. Sureda, D. Kataria, B. Belkouchi, A. Conte, S. Seminari, R. Villain, RF helicon-based plasma thruster (IPT): Design, set-up, and first ignition, 71st International Astronautical Congress, Online, The CyberSpace Edition (IAC-20,C4,5,11,x58032) (October 2020).

[42] V. Abrao Oiko, P. Roberts, A. Macario Rojas, S. Edmondson, S. Haigh, B. Holmes, S. Livadiotti, N. Crisp, K. Smith, L. Sinpetru, J. Becedas, R. Domínguez, V. Sulliotti-Linne, S. Christensen, T. Kauffman Jensen, J. Nielsen, M. Bisgaard, Y.-A. Chan, G. Herdrich, F. Romano, S. Fasoulas, C. Traub, D. Garcia-Almiñana, M. Garcia-Berenguer, S. Rodriguez-Donaire, M. Sureda, D. Kataria, B. Belkouchi, A. Conte, S. Seminari, R. Villain, Ground-based experimental facility for orbital aerodynamics research: Design, construction and characterisation, in: 71st International Astronautical Congress (IAC) – The CyberSpace Edition, 12-14 October 2020, 2020.

[43] N. Crisp, P. Roberts, S. Livadiotti, A. Macario Rojas, V. Oiko, S. Edmondson, S. Haigh, B. Holmes, L. Sinpetru, K. Smith, J. Becedas, R. Domínguez, V. Sulliotti-Linner, S. Christensen, J. Nielsen, M. Bisgaard, Y.-A. Chan, S. Fasoulas, G. Herdrich, F. Romano, C. Traub, D. García-Almiñana, S. Rodríguez-Donaire, M. Sureda, D. Kataria, B. Belkouchi, A. Conte,

S. Seminari, R. Villain, In-orbit aerodynamic coefficient measurements using SOAR (Satellite for Orbital Aerodynamics Research), Acta Astronautica 180 (2021) 85–99. doi:https://doi.org/10.1016/j.actaastro.2020.12.024.